

DEUP: Direct Epistemic Uncertainty Prediction

Moksh Jain ^{*1,2} Salem Lahlou ^{*1,3} Hadi Nekoei ¹ Victor Butoi ⁴ Paul Bertin ^{1,3} Jarrid Rector-Brooks ¹
Maksym Korablyov ^{1,3} Yoshua Bengio ^{1,3}

Abstract

Epistemic uncertainty is the part of out-of-sample prediction error due to the lack of knowledge of the learner. Whereas previous work was focusing on model variance, we propose a principled approach for directly estimating epistemic uncertainty by learning to predict generalization error and subtracting an estimate of aleatoric uncertainty, i.e., intrinsic unpredictability. This estimator of epistemic uncertainty includes the effect of model bias and can be applied in non-stationary learning environments arising in active learning or reinforcement learning. In addition to demonstrating these properties of Direct Epistemic Uncertainty Prediction (DEUP), we illustrate its advantage against existing methods for uncertainty estimation on downstream tasks including sequential model optimization and reinforcement learning. We also evaluate the quality of uncertainty estimates from DEUP for probabilistic classification of images and for estimating uncertainty about synergistic drug combinations.

1. Introduction

One of the remaining great challenges for machine learning research is that of purposeful knowledge-seeking by learning agents. A key ingredient in this long-term and important quest is the estimation of epistemic uncertainty, i.e., the part of the uncertainty that is due to lack of knowledge, and which could potentially be eliminated with enough data if the learner converges to a Bayes-optimal predictor. Epistemic uncertainty estimation is already a key ingredient in active learning and Bayesian optimization methods (Aggarwal et al., 2014; Frazier, 2018) as well as exploration in Reinforcement Learning (Kocsis & Szepesvári, 2006; Tang et al., 2017). Epistemic uncertainty thus tells us how much could be gained from learning around a particular area of state-space or input data space. How should we

measure it? Much previous work has focused on model variance (Gal & Ghahramani, 2016; Lakshminarayanan et al., 2017), i.e., how different are the functions compatible with the learner’s preferences and the data. However, this does not take into account bias, due only to the learner’s preferences. Instead we propose to measure epistemic uncertainty in terms of the loss the learner cares about. The total expected out-of-sample loss at a point can be decomposed into epistemic uncertainty and aleatoric uncertainty. Aleatoric uncertainty is output noise, the part of the error that is intrinsic to the distribution of interest (and independent of the choice of the learner), or the error which may be achieved by a Bayes-optimal predictor. Model bias is due to the finite capacity generally self-imposed to avoid overfitting or reduce computational costs, and can be reduced in the case of asymptotically optimal learners (universal approximators with capacity that increases with the number of examples). Fig. 1 illustrates with Gaussian Processes (GP) that model variance is not necessarily a good predictor of the reducible generalization error.

Because epistemic uncertainty aims at estimating a potential knowledge gain, we propose a definition of it which is the expected generalization error at a point x minus the aleatoric uncertainty at x , i.e., the gap in generalization error compared to a Bayes-optimal predictor, which could be reduced with enough data, especially in the vicinity of x . In order to estimate epistemic uncertainty, we thus propose DEUP, for Direct Epistemic Uncertainty Prediction, where we train a side learner (the uncertainty predictor) with an appropriate objective and training data in order to predict this generalization error at x . A prediction of epistemic uncertainty at x can thus be obtained either by training to predict the generalization error at x and then subtracting the estimated aleatoric uncertainty at x , or by training the uncertainty predictor to predict the difference between generalization error and aleatoric uncertainty at x .

An interesting potential advantage of the proposed approach, compared with model variance estimators, is that DEUP error predictors can be explicitly trained to care about, and calibrate for estimating generalization error for examples which may come from a distribution different from the distribution of most of the training examples, i.e., an out-of-distribution (OOD) setting. Such non-stationarities arise

^{*}Equal contribution ¹Mila ²Microsoft ³Université de Montréal ⁴Cornell University. Correspondence to: Moksh Jain <mokshjn00@gmail.com>, Salem Lahlou <salem-lahlou9@gmail.com>.

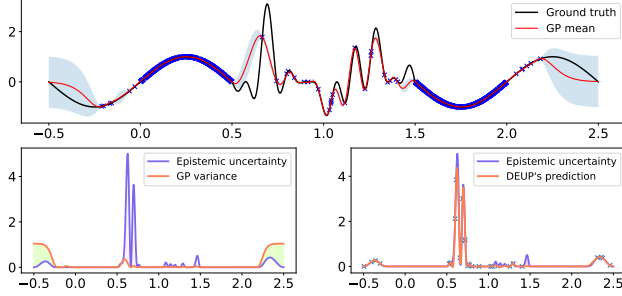


Figure 1. Top. A GP is trained on 1024 points in $[0, 0.5] \cup [1.5, 2]$, and 35 points in $[-0.25, 0] \cup [0.5, 1.5] \cup [2, 2.35]$. GP uncertainty (model standard deviation) in shaded blue. Bottom Left. Using GP variance as a proxy for epistemic uncertainty here misses out on important regions of the input space from which useful information can be acquired. Bottom right. With extra out-of-sample points, DEUP can learn an estimator of the epistemic uncertainty that captures that information. Using this estimator to make decisions (e.g. active learning) would focus on where more data could most reduce the loss. The experiments show realistic use cases of DEUP in which less (or no) additional data is required to obtain reasonable uncertainty estimators.

naturally in contexts like active learning and reinforcement learning (RL) because the learner explores new areas of the input space. We find that using variance estimators and density estimators as extra input features to the trained error predictor, such a calibration can be learned.

In this paper we thus consider two predictors: the main predictor (for the learning task of original interest) and an error predictor which can be used to predict epistemic uncertainty of the main predictor at given points, given some knowledge or estimate of aleatoric uncertainty. The proposed methodology can be seen as an end-to-end approach to epistemic uncertainty estimation, i.e., to help estimate where a learner would acquire the most information in terms of loss reduction. In order to select points with high epistemic uncertainty, one would still need some kind of search (in the space of x), e.g., to propose new candidates for active learning (Nguyen et al., 2019; Aggarwal et al., 2014) or sequential model optimization (Kushner, 1964; Jones et al., 1998; Snoek et al., 2012), or exploration in RL (Osband et al., 2016; Janz et al., 2019; Kocsis & Szepesvári, 2006).

In the non-stationary settings of active learning or RL, we typically want to retrain the main predictor as we acquire new training data, not just because more training data is generally better but also to better track the changing distribution. This setting makes it challenging to train the main predictor but it also entails an even greater non-stationarity when training the error predictor: a large error initially made at a point x before x is incorporated in the training set (along with an outcome y) will typically be greatly reduced after updating the main predictor with that example (x, y) . We

propose several strategies to cope with this non-stationarity, the most important being to rely on additional features (such as log-density estimates and model variance estimates at x) which capture information about the predictor and the dataset. These features account for variations in prediction error arising due to updates of the main predictor. Thus, incorporating such features as input to the error predictor makes its training distribution less non-stationary.

The experiments presented here explore first the scenario of purely trying to estimate epistemic uncertainty in terms of the recoverable generalization error, and second how this can be used in contexts of sequential model optimization and exploration in RL (where the issue of non-stationarity arises). The main contributions of this paper are thus the following:

1. Present a novel end-to-end approach to epistemic uncertainty estimation, the Direct Epistemic Uncertainty Prediction (DEUP) approach.
2. Show experimentally that this direct estimating of epistemic uncertainty can lead to more precise estimates than variance-based ones, especially when trying to learn functions which are more difficult to learn in some regions of space than others, and this is where bias would vary.
3. Propose means to mitigate the issue of non-stationarity arising in training the uncertainty estimates.
4. Validate the above in the contexts of (a) sequential model optimization and (b) exploration in RL.

2. Model Bias, Model Variance, Aleatoric Uncertainty and Epistemic Uncertainty

Let us define more formally some of the above concepts. Consider a learning algorithm \mathcal{L} mapping a dataset \mathcal{D}_n (with n indexing gradually larger datasets) to a predictive function $f = \mathcal{L}(\mathcal{D}_n)$. \mathcal{L} tries to minimize the expected value of a loss $l(f(x), y) \in \mathbb{R}$. Let $P(Y|x)$ denote the ground truth conditional distribution of outcomes Y at the given point x .

Definition 2.1 *The total uncertainty of f at x is defined as the expected loss of f at x under $P(Y|x)$:*

$$\mathcal{U}(f, x) = \int l(f(x), y) dP(y|x). \quad (1)$$

Definition 2.2 *A Bayes-optimal predictor f^* has the property that for every point x*

$$f^*(x) \in \arg \min_{\tilde{y}} \int l(\tilde{y}, y) dP(y|x). \quad (2)$$

Note how Bayes-optimal predictors only depend on the underlying data distribution and not on the learning algorithm \mathcal{L} or its resulting predictor f . Additionally, all predictors which are Bayes-optimal have the same total uncertainty for all x . Aleatoric uncertainty is the irreducible expected error, i.e., that made by a Bayes-optimal predictor:

Definition 2.3 We define **aleatoric uncertainty** at x as the total uncertainty of any Bayes-optimal predictor f^* at x :

$$\mathcal{A}(x) = \mathcal{U}(f^*, x). \quad (3)$$

and we note that by definition $\mathcal{A}(x) \leq \mathcal{U}(f, x), \forall f \forall x$.

We are now ready to propose a definition of epistemic uncertainty of a predictor f as the gap between the error of f at x and the lowest possible error at x , i.e., the part of the loss which could be reducible, given more knowledge.

Definition 2.4 We define epistemic uncertainty $\mathcal{E}(f, x)$ of a predictor f at x as

$$\mathcal{E}(f, x) = \mathcal{U}(f, x) - \mathcal{A}(x) = \mathcal{U}(f, x) - \mathcal{U}(f^*, x). \quad (4)$$

Another way to think about the epistemic uncertainty is to consider what happens to the learning algorithm \mathcal{L} when the number of training examples goes to infinity (by growing n). If \mathcal{L} is non-parametric, it means that it can increase its capacity as n increases. Examples of these include k -nearest neighbors with k increasing at a proper rate slower than n , and neural networks whose size and regularization are hyper-parameters optimized on a validation set. If this is done properly, then \mathcal{L} converges to a Bayes-optimal predictor:

Definition 2.5 A learning algorithm \mathcal{L} applied to a sequence of training sets \mathcal{D}_n whose elements converge in distribution is **asymptotically optimal** at x and for that sequence if

$$\lim_{n \rightarrow \infty} \mathcal{U}(\mathcal{L}(\mathcal{D}_n), x) = \mathcal{A}(x), \quad (5)$$

or equivalently

$$\lim_{n \rightarrow \infty} \mathcal{E}(\mathcal{L}(\mathcal{D}_n), x) = 0. \quad (6)$$

We can now indeed see that for asymptotically optimal learning algorithms, total uncertainty converges to aleatoric uncertainty, i.e., epistemic uncertainty is completely reducible.

Some learning algorithms, in particular those based on Bayesian approaches, maintain a set of possible solutions to the learning problem, along with a different weight or probability for each of them. This is conveniently represented by a probability distribution $P_{\mathcal{L}}(f(x)|\mathcal{D}_n)$ over solutions $f(x)$, often by maintaining a posterior distribution $P_{\mathcal{L}}(\theta|\mathcal{D}_n)$ over internal parameters θ , in the parametric setting, with the solutions $f_{\theta}(x)$ indexed by θ . It makes sense and has been the basis of previous work on epistemic uncertainty that measures of the disagreement between different $f_{\theta}(x)$, like their variance under $P_{\mathcal{L}}(f_{\theta}(x)|\mathcal{D}_n)$, give us information about epistemic uncertainty: if only one solution was deemed compatible with the data, the model would be certain, and if the solutions are very different from each other, the model would have a lot of uncertainty about the right answer. Furthermore, as $n \rightarrow \infty$, model variance, defined below, would go to 0 if the posterior over functions collapses to a Dirac.

Definition 2.6 For a learning algorithm \mathcal{L} which produces a distribution $P_{\mathcal{L}}(f(x)|\mathcal{D}_n)$ over possible solutions $f(x)$ at x , the **model variance** at x is defined as

$$\begin{aligned} V(\mathcal{L}, \mathcal{D}_n, x) &= \text{Var}_{P_{\mathcal{L}}(f(x)|\mathcal{D}_n)}(f(x)) \\ &= \int (f(x) - \bar{f}(x))^2 dP_{\mathcal{L}}(f(x)|\mathcal{D}_n) \end{aligned} \quad (7)$$

where $\bar{f}(x) = E_{P_{\mathcal{L}}(f(x)|\mathcal{D}_n)}[f(x)] = (\int f(x) dP_{\mathcal{L}}(f(x)|\mathcal{D}_n))$ is the mean answer and would be the default predictor of the learner if a single prediction is required. Note that the above definition makes sense for the squared error loss, but we can generalize it to a generic loss function (although the semantics of variance may be lost):

$$V(\mathcal{L}, \mathcal{D}_n, x) = \int l(f(x), \bar{f}(x)) dP_{\mathcal{L}}(f(x)|\mathcal{D}_n) \quad (8)$$

which coincides with the standard variance definition when $l(\hat{y}, y) = (\hat{y} - y)^2$.

Note that model variance is different from epistemic uncertainty as we defined it, and it does not tell us directly what the reducible gap in generalization error is. For example, it does not say anything about model bias due to the finite capacity of the learner, or for example its preference for smoother functions (e.g., with kernel-based Gaussian Processes), or its lack of degrees of freedom necessary to sufficiently fit the training data.

Definition 2.7 Following the standard decomposition of squared error in terms of noise plus bias plus variance, we define **model bias** as

$$B(\mathcal{L}, \mathcal{D}_n, x) = E_f[\mathcal{E}(f, x)] - V(\mathcal{L}, \mathcal{D}_n, x). \quad (9)$$

Note that with a GP, we typically use the mean function \bar{f} as predictor, and its epistemic uncertainty as we define it reduces to model bias and not to model variance:

Proposition 1 If $l(\hat{y}, y) = (\hat{y} - y)^2$, and the learning algorithm \mathcal{L} produces a distribution over possible solutions, with predictive mean \bar{f} , then:

$$\mathcal{E}(\bar{f}, x) = B(\mathcal{L}, \mathcal{D}_n, x) \quad (10)$$

The proof is given in Appendix B. As will be seen in Section 5.1.1 and illustrated in Fig. 1, the mismatch between variance predictors and the reducible error gap (our definition of epistemic uncertainty) can be substantial and matter for setups like active learning, sequential model optimization or RL.

2.1. Additional Properties: Negative Log-Likelihood and Squared Loss

Let us consider the special cases of the negative log-likelihood loss in general (for outputs which may be discrete

or continuous) and that of the squared error loss (which ends up being a special case of the former for normally distributed outputs). Below we see $Q(Y|x)$ as a probability mass or density function (over y), which is also a function of x .

Definition 2.8 *The negative log-likelihood (NLL) loss takes as first argument $Q(Y|x)$ a probability mass or density function and returns*

$$l_{NLL}(Q(Y|x), y) = -\log Q(Y = y|x). \quad (11)$$

Definition 2.9 *The mean squared error (MSE) loss or simply squared loss is*

$$l_{MSE}(\hat{y}, y) = (\hat{y} - y)^2. \quad (12)$$

Proposition 2 *For the NLL loss with ground truth $P(Y|x)$ and predictor $Q(Y|x)$, the total uncertainty $\mathcal{U}(Q(Y|x), x)$ is a cross-entropy, i.e.,*

$$\begin{aligned} \mathcal{U}(Q(Y|.), x) &= CE(P(Y|x)||Q(Y|x)) \\ &= - \int dP(y|x) \log Q(y|x) \end{aligned} \quad (13)$$

which is shown by applying the definitions.

Proposition 3 *For the NLL loss with ground truth $P(Y|x)$, the aleatoric uncertainty $\mathcal{A}(x)$ in this setting is the entropy $H[P(Y|x)]$ of the ground truth conditional:*

$$\mathcal{A}(x) = - \int dP(y|x) \log P(y|x) = H[P(Y|x)], \quad (14)$$

shown from the cross-entropy $CE(P(Y|x)||Q(Y|x))$ being minimized when $Q = P$.

Proposition 4 *For the NLL loss with ground truth $P(Y|x)$ and predictor $Q(Y|x)$, the epistemic uncertainty $\mathcal{E}(Q(Y|x), x)$ is the Kullback-Liebler divergence between P and Q (with P as the reference):*

$$\begin{aligned} \mathcal{E}(Q(Y|.), x) &= KL(P(Y|x)||Q(Y|x)) \\ &= \int dP(y|x) \log \frac{P(y|x)}{Q(y|x)} \end{aligned} \quad (15)$$

which is shown by combining the above two propositions and the definition of epistemic uncertainty.

To move towards the MSE loss, consider the special case of NLL with a conditionally Normal output density for both P and Q .

Proposition 5 *For the NLL loss with a conditionally Normal output density for both P and Q , with respective means $f^*(x)$ and $f(x)$ and respective variances $\sigma_P^2(x)$ and $\sigma_Q^2(x)$, the epistemic uncertainty is*

$$\begin{aligned} \mathcal{E}(Q(Y|.), x) &= \frac{1}{2\sigma_Q^2(x)} l_{MSE}(f(x), f^*(x)) \\ &\quad + KL(P(Y|x)||\tilde{Q}(Y|x)), \end{aligned} \quad (16)$$

where $\tilde{Q}(\cdot|x)$ is obtained by shifting $Q(\cdot|x)$ towards $P(\cdot|x)$ (i.e., $\tilde{Q}(\cdot|x)$ is Gaussian with mean $f^*(x)$ and variance $\sigma_Q^2(x)$), and the Bayes-optimal mean predictor is $f^*(x) = E_P[Y|x]$. Note that if $\sigma_P = \sigma_Q$, then the KL term is zero.

The proof is presented in Appendix B. We can compare with the MSE loss (which assumes a constant variance $\sigma = \sigma_P = \sigma_Q$) and obtain the same result up to variance scaling.

Proposition 6 *For the MSE loss we obtain $\mathcal{E}(f, x) = l_{MSE}(f(x), f^*(x))$, $\mathcal{U}(f, x) = E[l_{MSE}(f(x), Y)]$, and $\mathcal{A}(x) = E[l_{MSE}(f^*(x), Y)]$, as shown in Appendix B.*

3. Direct Epistemic Uncertainty Prediction

The core principle of DEUP (Direct Epistemic Uncertainty Prediction) is to **use observed out-of-sample errors in order to train an error predictor which can be used to estimate epistemic uncertainty elsewhere**. These may be in-distribution or out-of-distribution errors, depending on whichever we care about.

3.1. Fixed Training Set

We first consider the simpler scenario with a fixed training set \mathcal{D}_n on which a learning algorithm \mathcal{L} has been applied to obtain a predictor $f_{\mathcal{L}(\mathcal{D}_n)}$ (or just f for short, since n and \mathcal{D}_n are fixed). We assume that some out-of-sample (validation) data has been set aside and can thus be used for training an error predictor. If the aleatoric uncertainty is known to be zero or near zero, then predicting epistemic uncertainty boils down to predicting the out-of-sample loss of the main predictor f at x .

Proposition 7 *Training an error predictor e with (input,target) pairs $(x, l(f(x), y))$ and squared loss makes e estimate the total uncertainty $\mathcal{U}(f, x) = E[l(f(x), Y)]$, and if e 's learner is asymptotically optimal, then $e(x) \rightarrow \mathcal{U}(f, x)$ for all x , as the amount of validation data goes to infinity. Proven in Appendix B.*

If $\mathcal{A}(x) = 0$ then $e(x)$ is an estimator of $\mathcal{E}(f, x)$ as well as of $\mathcal{U}(f, x)$. If an estimator $a(x)$ of aleatoric uncertainty is available, then $e(x) - a(x)$ becomes an estimator of epistemic uncertainty at x . Alternatively, one could train e with examples $(x, l(f(x), y) - a(x))$ and also obtain an estimator of epistemic uncertainty.

3.2. Estimating Aleatoric Uncertainty

3.2.1. HOMOSCEDASTIC CASE

If $\mathcal{A}(x)$ is a constant A , then it is the expected loss (over some $P(x)$ distribution) of the Bayes-optimal predictor. For asymptotically optimal learners, plotting the decreasing test error as a function of increasing n should have A as asymptote. While the in-sample average error (average training loss) is also an estimator of the expected test loss, it is biased

by the generalization gap and thus generally underestimates the Bayes-optimal generalization error.

3.2.2. ACCESS TO AN ORACLE

There is a broad special case which is relevant in active learning scenarios, where one has access to an oracle from which we can obtain samples of $Y \sim P(Y|x)$ at any given point x . In that case, one can train an estimator $a(x)$ of aleatoric uncertainty by obtaining pairs of samples Y_1 and Y_2 at the same x , for a set of representative x 's.

Proposition 8 *Let l be the square loss, $y_1 \sim P(Y|x)$ and $y_2 \sim P(Y|x)$ be a pair of outcomes at x . Training predictor $a(x)$ with the squared loss on (input,target) examples $(x, \frac{1}{2}(y_1 - y_2)^2)$ makes $a(x)$ an estimator of $\mathcal{A}(x)$, and if the learning algorithm for a is asymptotically optimal, it converges to \mathcal{A} . Proven in Appendix B.*

3.3. Retraining with Novel Examples

Interactive settings are more interesting but more challenging, e.g., epistemic uncertainty estimation is used in order to acquire information and iteratively gather new examples. In sequential model optimization, the objective is to optimize an unknown function, and the learner can iteratively query an oracle at chosen x 's. Higher epistemic uncertainty at x is a clue that learning more about x would help the learner, as illustrated in our experiments (Figures 3 and 4) where good epistemic uncertainty estimation translates in faster learning curves. However, this interactive setting also raises significant challenges: the main predictor is going to be retrained multiple times, with the new examples being added to the observed data each time.

Two kinds of non-stationarities arise here. First, new examples are not arising independently (since their choice depends on the epistemic uncertainty estimation obtained from earlier examples). This makes the stream of data seen by the main predictor non-stationary - for example in sequential model optimization or RL, the new examples may concentrate more and more towards regions where the reward might be higher. Second, the error predictor itself faces even more non-stationarities, even if the data stream seen by the main predictor was i.i.d.. Indeed, after example x was selected the main predictor will then be retrained using that additional data and this will typically yield a much lower epistemic uncertainty at x .

3.3.1. FACING NON-STATIONARITY DUE TO EXPLORATION

The first kind of non-stationarity described above is due to the very process of exploration and affects both the main predictor and the error predictor. Whereas it is not clear how variance-based predictors can cope with this, DEUP can in principle cope with it by virtue of having the error predictor trained not on out-of-sample and in-distribution examples but on out-of-sample and out-of-distribution examples of

the kind we care about (e.g., as obtained from the interactive learning process). The error predictor then learns to predict the error which would be made on typical new examples coming from what we may call by analogy the "frontier of knowledge", while this frontier continuously expands due to exploration and learning. Note how this OOD error will tend to be higher than if the examples were in-distribution and how DEUP's training procedure can in principle capture some of this gap by learning to predict OOD errors due to that interactive learning process.

3.3.2. FACING NON-STATIONARITY DUE TO RETRAINING

The more challenging non-stationarity however arises because of retraining, which completely changes the epistemic uncertainty at the points newly added to the training set. If we only consider (input,error) pairs (x_t, e_t) to train the error predictor, then we get a sequence of points which really come from very different distributions, and the older examples (previously seen by the main predictor) should not have an error e_t but a much lower one (maybe 0). To get rid of that source of non-stationarity, we have to include additional inputs which explain why the error is different before and after example t has been added to the training set of the main predictor. In principle, we could consider tuples $(x_t, \mathcal{L}, \mathcal{D}_t, e_t)$ for this purpose. However, \mathcal{L} is fixed throughout and can thus be ignored. With \mathcal{D} a very high-dimensional object and the number of acquired points sometimes small in active learning or sequential model optimization, we may face an overfitting problem when training the error predictor. Hence in this paper, we propose to use **stationarizing features** of \mathcal{D} , $\phi_{\mathcal{D}}(x_t)$, as inputs to the error predictor at x_t (and proxies for capturing the variations of \mathcal{D} as they pertain to x_t). The stationarized (input,error) training examples for the error predictor are thus $((x_t, \phi_{\mathcal{D}_t}(x_t)), e_t)$ for example t .

3.3.3. STATIONARIZING FEATURES

In this paper we explored the use of two scalar features to stationarize the training set of the error predictor: a model variance estimate and a log-density estimate. Both have been used in the past as proxies for epistemic uncertainty. It is well established that when a new x_t does not look like the training examples, as captured by the differences in log-densities or variances, it is more likely to yield a larger prediction error. Interestingly, humans appear to use familiarity (Kasperson et al., 1988) as a strong clue for estimating risk (which is closely related to uncertainty). We use a density estimator evaluated at x_t , trained on the input part of the data \mathcal{D}_{t-1} , i.e., before x_t is incorporated in it. For numerical reasons, we used $\log \hat{q}(x_t | \mathcal{D}_{t-1})$ as our second feature, where \hat{q} is thus obtained by training a third model as density estimator (such as a kernel density estimator or a flow-based deep network (Rezende & Mohamed, 2015), in our case). Like the other predictors, the density learner

also needs to be fine-tuned when new data are added to its training set.

3.3.4. MAKING A BALANCED DATA SET INCLUDING LOW ERROR ON IN-SAMPLE POINTS

What is the epistemic uncertainty at x_t after it has been incorporated in the main predictor’s training set? With this quantity, we could form an additional training example for the error predictor, forcing it to output a smaller value at x_t when the features $\phi_{\mathcal{D}_t}(x_t)$ tell it that x_t has been seen. For this purpose, we can begin by incorporating in the error predictor an extra binary input feature s_i , which distinguishes seen examples from unseen examples: for any x_i except the most recently acquired example, there could be two training examples for the error predictor, one with this binary feature $s_i = 0$ (before x_i was trained on) and one with $s_i = 1$ (after x_i was trained on). The density and variance estimators (used as input features of the error predictor) would also be different for these two examples, as they would reflect the values of these features respectively before and after x_i was added to \mathcal{D} . The estimated density should also change significantly after x_i is incorporated in \mathcal{D} . In our experiments we use the in-sample error at x_i as a target proxy for these in-sample examples, thus yielding the following pair of (input, target) examples for the error predictor:

$$\begin{aligned} \text{input} &= (x_i, 0, \log \hat{q}(x_i|\mathcal{D}_{i-1}), \hat{V}(\mathcal{L}, \mathcal{D}_{i-1}, x_i)), \\ \text{target} &= l(\mathcal{L}(\mathcal{D}_{i-1})(x_i), y_i)) \\ \text{input} &= (x_i, 1, \log \hat{q}(x_i|\mathcal{D}_i), \hat{V}(\mathcal{L}, \mathcal{D}_i, x_i)), \\ \text{target} &= l(\mathcal{L}(\mathcal{D}_i)(x_i), y_i)) \end{aligned} \quad (17)$$

where $\hat{q}(x|\mathcal{D})$ is an input density estimate from data \mathcal{D} at x , and $\hat{V}(\mathcal{L}, \mathcal{D}, x)$ is a model variance estimate at x (when the learner is trained with \mathcal{D}). In the case of the squared error loss, we found that using the logarithm of the squared error as target works better in some settings.

4. Related Work

Kiureghian & Ditlevsen (2009) characterized the sources of uncertainty as aleatoric (inherent noise) and epistemic (incomplete knowledge). Gaussian Processes or GPs (Williams & Rasmussen, 1995), provide a way to capture epistemic uncertainty through the disagreement between the different predictors that fit the data. In Deep Learning, Kendall & Gal (2017), Blundell et al. (2015) and Depeweg et al. (2018) use the posterior distribution of network weights (MacKay, 1992) in Bayesian Neural Networks (BNNs) to capture epistemic uncertainty. Other techniques that rely on measuring the discrepancy between different predictors as a proxy for epistemic uncertainty include MC-Dropout (Gal & Ghahramani, 2016), that interprets Dropout (Hinton et al., 2012) as a variational inference technique in BNNs. These

approaches, because they rely on sampling multiple sets of weights or dropout masks at inference time, share some similarities with ensemble-based methods, that include bagging (Breiman, 1996) and boosting (Efron & Tibshirani, 1994), in which multiple predictors are trained, and used jointly to make a prediction. For example, Shaker & Hüllermeier (2020) use Random Forests (Breiman, 2001) to estimate epistemic uncertainty. Deep Ensembles (Lakshminarayanan et al., 2017) follow the same principle and use ensembles of neural networks. In addition to this, several other variants of this central idea of measuring discrepancy between different predictors have been proposed recently (Amini et al., 2020; Tagasovska & Lopez-Paz, 2019; Liu et al., 2020; van Amersfoort et al., 2020; Wen et al., 2020; Antoran et al., 2020). We discuss these methods in more detail in Appendix A

More closely related to DEUP, Yoo & Kweon (2019) proposed a loss prediction module for learning to predict the value of loss function. Hu et al. (2020) also propose using a separate network that learns to predict the variance of an ensemble. These methods, however, are trained only to capture the in-sample error, and do not capture the out-of-sample error which is more relevant for scenarios like active learning where we want to pick x where the reducible generalization error is large. EpiOut (Umlauft et al., 2020) and Hafner et al. (2019) propose learning a binary output that simply captures low or high epistemic uncertainty, which can be insufficient in settings which require more nuance than a high/low prediction.

5. Experiments

5.1. Uncertainty Estimation

5.1.1. IMPORTANCE OF EPISTEMIC UNCERTAINTY CALIBRATION

In tasks that use uncertainty estimates to make decisions, and when the resources are limited, it is important to have well calibrated uncertainty estimates, to avoid exploring uninteresting areas of the search space, as we will observe in the following subsections. In order to show why relying on variance estimates alone as a proxy for epistemic uncertainty might hurt the performances on these tasks, we design a function with varying degrees of smoothness (as measured by the absolute values of its derivatives), and use fewer training points in the less smooth regions. We consider the scenario described in Section 3.1, where the task is to regress a known one-dimensional function.

In Figure 1, we use a GP as a predictor, and compare the GP’s variance to the epistemic uncertainty (which is equal to the square loss between the GP’s predicted mean and the ground truth, as per Proposition 6). The figure shows that, naturally, in regions of the input space where little or no data is available, and especially in the less smooth regions, the predicted variance underestimates the epistemic uncertainty

(squared error) by a higher margin compared to the other regions. We see that training another GP to directly estimate this squared loss, using a small held out out-of-sample data set for which the ground truth value is known, allows to close the gap between the predicted uncertainty and the true epistemic uncertainty. Note that this second predictor can be the output of any learning algorithm \mathcal{L} .

Naturally, if we had access to the held out set in the active learning setting, it would be wiser to use it as part of the training set of the main predictor, rather than the uncertainty predictor. In active learning, it is the acquired points, before they are used to retrain the main predictor, that play the role of the out-of-sample examples to train DEUP. Thanks to the stationarizing features introduced in Section 3.3, these acquired points should be informative enough for DEUP to generalize its uncertainty estimates to unknown regions of the search space, and use these estimates to help the learner to acquire new points. In RL, because the targets (e.g. of Q-Learning) are themselves estimates of the true targets, all data seen at any particular point is in principle out-of-sample and is informative for the uncertainty estimator, when the inputs are used in conjunction with the stationarizing features.

Table 1. Spearman Rank Correlation between predicted uncertainty and the true generalization error on OOD data (SVHN) with models (3 seeds) trained on CIFAR-10. DEUP significantly outperforms the baselines.

Model	ResNet-18	ResNet-50
MC-Dropout	28.72 ± 0.02	31.22 ± 0.03
Deep Ensemble	38.08 ± 0.04	40.09 ± 0.04
DUQ	37.56 ± 0.03	39.88 ± 0.03
DEUP	42.45 ± 0.04	45.71 ± 0.02

5.1.2. EPISTEMIC UNCERTAINTY PREDICTIONS FOR REJECTING DIFFICULT EXAMPLES

Epistemic uncertainty estimates can be used to reject difficult examples where the predictor might fail, such as OOD inputs. With this objective, we consider a variant of the standard OOD Detection task (van Amersfoort et al., 2020), where we train ResNets (He et al., 2016) for CIFAR-10 classification (Krizhevsky, 2009) and aim to reject high error OOD examples. To facilitate rejection of examples of classes other than those in the training set, we use a Bernoulli Cross-Entropy Loss for each class (van Amersfoort et al., 2020): $l(f(x), y) = -\sum_i y_i \log f_i(x) + (1 - y_i) \log(1 - f_i(x))$ where y is a one-hot vector ($y_i = 1$ if i is the correct class, and 0 otherwise), $f_i(x)$ indicates the probability for class i predicted by the model. This allows us to naturally define a label for out-of-distribution data, $y = \{0, \dots, 0\}$. To ascertain how well an epistemic error estimate sorts examples in terms of their NLL, we consider the rank correlation between the predicted uncertainty and the observed generalization error on OOD samples from

SVHN (Netzer et al., 2011). This metric focuses on the quality of the uncertainty estimates rather than just their ability to simply classify in- vs out-of-distribution examples. Further details of the experimental setup are discussed in Appendix D. Table 1 shows that DEUP’s uncertainty predictions have high rank correlation with the underlying generalization errors, compared with the baselines. Note that we ignore the effect of aleatoric uncertainty (due to human labeling error), measuring which would require a specifically designed human study.

Table 2. Comparison of uncertainty estimation quality for different models on a test set. *Corr. w. res.* shows the correlation between model residuals and predicted uncertainties $\hat{\sigma}$. *Upper Bound* refers to the correlation between $\hat{\sigma}$ and true samples from $\mathcal{N}(0, \hat{\sigma})$. *Ratio* is the ratio between col. 1 and 2. Results are averaged over 3 seeds.

Model	Corr. w. res.	U. Bound	Ratio
MC-Dropout	0.14 ± 0.07	0.56 ± 0.05	0.25 ± 0.12
Deep Ensemble	0.30 ± 0.09	0.59 ± 0.04	0.50 ± 0.13
In-Sample	0.32 ± 0.09	0.62 ± 0.06	0.52 ± 0.14
DEUP	0.47 ± 0.03	0.63 ± 0.05	0.75 ± 0.07

5.1.3. EPISTEMIC UNCERTAINTY ESTIMATION FOR DRUG COMBINATIONS

To validate DEUP’s uncertainty estimates in a real-world setting, we measured its performance on a regression task predicting the synergy of drug combinations. Estimating uncertainty in the context of drug combination experiments is an important step towards building models that can drive the exploration of the drug combination space. As shown in Table 2, the out-of-sample error predicted by DEUP correlates better with residuals of the model on the test set in comparison to several other uncertainty estimation methods, including an estimator of the in-sample error. Moreover, DEUP can better capture the order of magnitude of the residuals as shown in Figure 2. Details on our experimental setup are provided in appendix H.

5.2. Sequential Model Optimization

In sequential model optimization, the choice of which example to query in order to improve the model should be based on both predicted values (we are trying to maximize the unknown function) and predicted uncertainties (higher uncertainty offers the opportunity of discovering yet higher values of the function). Acquisition functions, such as Upper Confidence Bound (UCB, Srinivas et al. (2010)) and Expected Improvement (EI, Močkus (1975)) handle this trade-off between exploration and exploitation, and one can select the next candidate, or next batch of candidates, by looking for x maximizing the acquisition function. In this section, we demonstrate that we can use a neural net regressor as a model for the unknown function, along with DEUP to estimate epistemic uncertainty. To optimize the acquisition function, we treat the main predictor and DEUP epistemic uncertainty prediction as mean and variance of

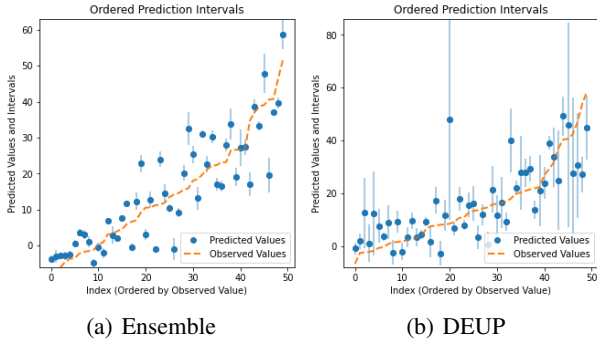


Figure 2. Predicted mean and uncertainty on a test set. 50 examples from the test set are ordered by increasing value of true synergy score (orange). Model predictions and uncertainties are visualized in blue. Ensemble (and MC-dropout, not shown) consistently underestimated the uncertainty while DEUP seems to capture the right order of magnitude.

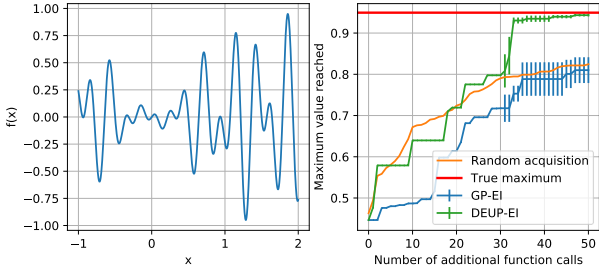


Figure 3. Left: function to optimize. Right: maximum value reached by the different methods. The error bars represent the standard error across 5 different runs, with different initial sets of 6 pairs. For clarity, the error bars are omitted in the initial stages of optimization, and for the random acquisition curve. The plots for MC-Dropout-EI and Ensemble-EI are omitted for clarity, as their final performances are under 0.65, and are shown in Appendix F instead. In each run, all the methods start with the same initial set of 6 points. GP-EI tends to get stuck in local optima and requires more than 50 steps, on average, to reach the global maximum.

a Gaussian distribution representing the learner’s current knowledge of the function to optimize. We find that DEUP-EI outperforms GP-EI, an established baseline (Bull, 2011), as well as neural networks with MC-Dropout or Ensembles to estimate model variance, in different optimization tasks.

In Figure 3, we optimize a synthetic function with one-dimensional inputs. The function is designed to have multiple local maxima. DEUP-EI is the only method that consistently reaches the global maximum in under 50 optimization steps (56 calls to the oracle in total). Experimental details, along with comparative results on a two-dimensional function that illustrate how DEUP outperforms the other methods, are shown in Appendix F.

5.3. Reinforcement Learning

Similar to sequential model optimization, a key challenge in reinforcement learning (RL) is efficient exploration of the input state space. To investigate the effectiveness of

DEUP’s uncertainty estimates in the context of RL, we incorporate epistemic uncertainties predicted by DEUP to DQN (Mnih et al., 2013), which we refer to as DEUP-DQN. Specifically, we train the uncertainty predictor with the objective to predict the TD-error, using log-density as a stationarizing input. The predicted uncertainties are then used as an exploration bonus in the Q-values. Details of the experimental setup are in Appendix G.

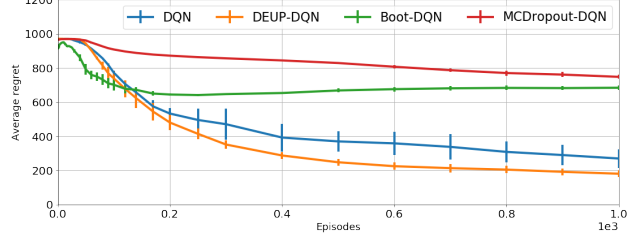


Figure 4. Average regret on CartPole task. The error bars represent the standard error across 5 different runs.

We evaluate DEUP-DQN on CartPole, a classic RL task, from *bsuite* (Osband et al., 2020), against DQN + ϵ -greedy, DQN + MC-Dropout (Gal & Ghahramani, 2016) and Bootstrapped DQN (Osband et al., 2016). Figure 4 shows that DEUP is able to achieve much lower regret compared to all the baselines, which demonstrates the advantage of DEUP’s uncertainty estimates for efficient exploration.

6. Conclusion and Future Work

In the case that aleatoric uncertainty can be estimated, one can quantitatively evaluate different predictors of epistemic uncertainty in terms of their ability to predict out-of-sample (or even better, out-of-distribution) errors at given points. This paper introduces DEUP, an end-to-end approach to training such error predictors by minimizing the losses made by the error predictor. Whereas previous work on epistemic uncertainty focused on model variance, DEUP directly estimates the reducible generalization error and thus takes into account model bias due to finite capacity or regularization. Although the idea is simple, it raises several challenges in the contexts where one wants to use the epistemic error predictors to drive the acquisition of new examples, yielding a sequence of datasets and corresponding retraining stages. We propose several ways to reduce the non-stationarity of the data seen by the error predictor. Comparative experimental results against standard epistemic uncertainty predictors confirm the usefulness of DEUP, either in estimating this reducible error or in downstream tasks like sequential model optimization and reinforcement learning with exploration.

This paper mostly focused on epistemic uncertainty but relies on some estimator of aleatoric uncertainty, and beyond the case where an oracle is available, exploited in the experiments, more work on aleatoric uncertainty estimation is warranted in the future.

Acknowledgements

The authors would like to thank Tristan Deleu, Anirudh Goyal, Doina Precup, Pierre Luc-Bacon, John Bradshaw, and José Miguel Hernández-Lobato for useful comments. This research was enabled in part by support provided by [Compute Canada](#), the Bill & Melinda Gates Foundation, IVADO and a CIFAR AI Chair.

References

Aggarwal, C. C., Kong, X., Gu, Q., Han, J., and Philip, S. Y. Active learning: A survey. In *Data Classification: Algorithms and Applications*, pp. 571–605. CRC Press, 2014.

Amini, A., Schwarting, W., Soleimany, A., and Rus, D. Deep evidential regression. In *Neural Information Processing Systems (NeurIPS)*, 2020.

Antoran, J., Allingham, J., and Hernández-Lobato, J. M. Depth uncertainty in neural networks. In *Neural Information Processing Systems (NeurIPS)*, 2020.

Balandat, M., Karrer, B., Jiang, D. R., Daulton, S., Letham, B., Wilson, A. G., and Bakshy, E. BoTorch: A Framework for Efficient Monte-Carlo Bayesian Optimization. In *Advances in Neural Information Processing Systems 33*, 2020. URL <http://arxiv.org/abs/1910.06403>.

Ballester, P. J. and Mitchell, J. B. A machine learning approach to predicting protein–ligand binding affinity with applications to molecular docking. *Bioinformatics*, 26(9):1169–1175, 2010.

Blundell, C., Cornebise, J., Kavukcuoglu, K., and Wierstra, D. Weight uncertainty in neural network. In *International Conference on Machine Learning*, pp. 1613–1622. PMLR, 2015.

Breiman, L. Bagging predictors. *Machine learning*, 24(2): 123–140, 1996.

Breiman, L. Random forests. *Machine learning*, 45(1): 5–32, 2001.

Bull, A. D. Convergence rates of efficient global optimization algorithms. *Journal of Machine Learning Research*, 12(10), 2011.

Cihlar, T. and Fordyce, M. Current status and prospects of hiv treatment. *Current opinion in virology*, 18:50–56, 2016.

Depeweg, S., Hernandez-Lobato, J.-M., Doshi-Velez, F., and Udluft, S. Decomposition of uncertainty in bayesian deep learning for efficient and risk-sensitive learning. In *International Conference on Machine Learning*, pp. 1184–1193. PMLR, 2018.

Dusenberry, M. W., Jerfel, G., Wen, Y., Ma, Y., Snoek, J., Heller, K., Lakshminarayanan, B., and Tran, D. Efficient and scalable bayesian neural nets with rank-1 factors. In *International Conference on Machine Learning (ICML)*, 2020.

Efron, B. and Tibshirani, R. J. *An introduction to the bootstrap*. CRC press, 1994.

Farquhar, S., Gal, Y., and Rainforth, T. On statistical bias in active learning: How and when to fix it. *ICLR’2021, arXiv:2101.11665*, 2021.

Frazier, P. I. A tutorial on bayesian optimization, 2018.

Gal, Y. and Ghahramani, Z. Dropout as a bayesian approximation: Representing model uncertainty in deep learning. In *International Conference on Machine Learning (ICML)*, pp. 1050–1059. PMLR, 2016.

Hafner, D., Tran, D., Lillicrap, T., Irpan, A., and Davidson, J. Noise contrastive priors for functional uncertainty. In *Conference on Uncertainty in Artificial Intelligence (UAI)*, 2019.

He, K., Zhang, X., Ren, S., and Sun, J. Deep residual learning for image recognition. In *Proceedings of the IEEE conference on computer vision and pattern recognition*, pp. 770–778, 2016.

Hinton, G. E., Srivastava, N., Krizhevsky, A., Sutskever, I., and Salakhutdinov, R. R. Improving neural networks by preventing co-adaptation of feature detectors. *arXiv preprint arXiv:1207.0580*, 2012.

Hu, S., Pezzotti, N., and Welling, M. A new perspective on uncertainty quantification of deep ensembles. *arXiv*, 2020.

Izmailov, P., Podoprikin, D., Garipov, T., Vetrov, D., and Wilson, A. Averaging weights leads to wider optima and better generalization. In *Conference on Uncertainty in Artificial Intelligence (UAI)*, 2018.

Janz, D., Hron, J., Mazur, P., Hofmann, K., Hernández-Lobato, J. M., and Tschiatschek, S. Successor uncertainties: Exploration and uncertainty in temporal difference learning. In *Neural Information Processing Systems (NeurIPS)*, 2019.

Jones, D. R., Schonlau, M., and Welch, W. J. Efficient global optimization of expensive black-box functions. *Journal of Global optimization*, 13(4):455–492, 1998.

Kasperson, R. E., Renn, O., Slovic, P., Brown, H. S., Emel, J., Goble, R., Kasperson, J. X., and Ratick, S. The social amplification of risk: A conceptual framework. *Risk analysis*, 8(2):177–187, 1988.

Kendall, A. and Gal, Y. What uncertainties do we need in bayesian deep learning for computer vision? In *Neural Information Processing Systems (NeurIPS)*, 2017.

Kingma, D. P. and Ba, J. Adam: A method for stochastic optimization. In *International Conference for Learning Representations*, 2015.

Kiureghian, A. D. and Ditlevsen, O. Aleatory or epistemic? does it matter? *Structural Safety*, 31(2):105–112, 2009. ISSN 0167-4730. doi: <https://doi.org/10.1016/j.strusafe.2008.06.020>. Risk Acceptance and Risk Communication.

Kocsis, L. and Szepesvári, C. Bandit based monte-carlo planning. In *In: ECML-06. Number 4212 in LNCS*, pp. 282–293. Springer, 2006.

Krizhevsky, A. Learning multiple layers of features from tiny images. Technical report, University of Toronto, 2009.

Kushner, H. J. A new method of locating the maximum point of an arbitrary multipeak curve in the presence of noise. *Journal of Basic Engineering*, 86:97–106, 1964.

Lakshminarayanan, B., Pritzel, A., and Blundell, C. Simple and scalable predictive uncertainty estimation using deep ensembles. In *Neural Information Processing Systems (NeurIPS)*, 2017.

LeCun, Y., Bottou, L., Bengio, Y., and Haffner, P. Gradient-based learning applied to document recognition. *Proceedings of the IEEE*, 86(11):2278–2324, 1998.

Liu, J. Z., Lin, Z., Padhy, S., Tran, D., Bedrax-Weiss, T., and Lakshminarayanan, B. Simple and principled uncertainty estimation with deterministic deep learning via distance awareness. In *Neural Information Processing Systems (NeurIPS)*, 2020.

MacKay, D. J. A practical bayesian framework for backpropagation networks. *Neural computation*, 4(3):448–472, 1992.

Maddox, W., Garipov, T., Izmailov, P., Vetrov, D., and Wilson, A. G. A simple baseline for bayesian uncertainty in deep learning. In *Neural Information Processing Systems (NeurIPS)*, 2019.

Malyutina, A., Majumder, M. M., Wang, W., Pessia, A., Heckman, C. A., and Tang, J. Drug combination sensitivity scoring facilitates the discovery of synergistic and efficacious drug combinations in cancer. *PLoS computational biology*, 15(5):e1006752, 2019.

Mnih, V., Kavukcuoglu, K., Silver, D., Graves, A., Antonoglou, I., Wierstra, D., and Riedmiller, M. Playing atari with deep reinforcement learning. *arXiv preprint arXiv:1312.5602*, 2013.

Močkus, J. On bayesian methods for seeking the extremum. In *Optimization techniques IFIP technical conference*, pp. 400–404. Springer, 1975.

Mokhtari, R. B., Homayouni, T. S., Baluch, N., Morgatskaya, E., Kumar, S., Das, B., and Yeger, H. Combination therapy in combating cancer. *Oncotarget*, 8(23):38022, 2017.

Morgan, H. L. The generation of a unique machine description for chemical structures-a technique developed at chemical abstracts service. *Journal of Chemical Documentation*, 5(2):107–113, 1965.

Netzer, Y., Wang, T., Coates, A., Bissacco, A., Wu, B., and Ng, A. Y. Reading digits in natural images with unsupervised feature learning. In *Advances in Neural Information Processing Systems (NIPS)*, 2011.

Nguyen, V.-L., Destercke, S., and Hüllermeier, E. Epistemic uncertainty sampling. In *International Conference on Discovery Science*, pp. 72–86. Springer, 2019.

Organization, W. H. and Initiative, S. T. *Treatment of tuberculosis: guidelines*. World Health Organization, 2010.

Osband, I., Blundell, C., Pritzel, A., and Van Roy, B. Deep exploration via bootstrapped dqn. *arXiv preprint arXiv:1602.04621*, 2016.

Osband, I., Doron, Y., Hessel, M., Aslanides, J., Sezener, E., Saraiva, A., McKinney, K., Lattimore, T., Szepesvári, C., Singh, S., Van Roy, B., Sutton, R., Silver, D., and van Hasselt, H. Behaviour suite for reinforcement learning. In *International Conference on Learning Representations*, 2020. URL <https://openreview.net/forum?id=rygf-kSYwH>.

Papamakarios, G., Pavlakou, T., and Murray, I. Masked autoregressive flow for density estimation. In *Neural Information Processing Systems (NeurIPS)*, 2017.

Rezende, D. and Mohamed, S. Variational inference with normalizing flows. In *International Conference on Machine Learning (ICML)*, pp. 1530–1538. PMLR, 2015.

Shaker, M. H. and Hüllermeier, E. Aleatoric and epistemic uncertainty with random forests. In *International Symposium on Intelligent Data Analysis*, pp. 444–456. Springer, 2020.

Snoek, J., Larochelle, H., and Adams, R. P. Practical bayesian optimization of machine learning algorithms.

In *Neural Information Processing Systems (NeurIPS)*, 2012.

Srinivas, N., Krause, A., Kakade, S. M., and Seeger, M. Gaussian process optimization in the bandit setting: No regret and experimental design. In *International Conference on Machine Learning (ICML)*, 2010.

Subramanian, A., Narayan, R., Corsello, S. M., Peck, D. D., Natoli, T. E., Lu, X., Gould, J., Davis, J. F., Tubelli, A. A., Asiedu, J. K., et al. A next generation connectivity map: L1000 platform and the first 1,000,000 profiles. *Cell*, 171(6):1437–1452, 2017.

Tagasovska, N. and Lopez-Paz, D. Single-model uncertainties for deep learning. In *Neural Information Processing Systems (NeurIPS)*, 2019.

Tang, H., Houthooft, R., Foote, D., Stooke, A., Chen, X., Duan, Y., Schulman, J., De Turck, F., and Abbeel, P. # exploration: A study of count-based exploration for deep reinforcement learning. In *Neural Information Processing Systems (NeurIPS)*, 2017.

Umlauft, J., Lederer, A., Beckers, T., and Hirche, S. Real-time uncertainty decomposition for online learning control. *ArXiv*, abs/2010.02613, 2020.

van Amersfoort, J. R., Smith, L., Teh, Y., and Gal, Y. Simple and scalable epistemic uncertainty estimation using a single deep deterministic neural network. In *International Conference on Machine Learning (ICML)*, 2020.

Wen, Y., Tran, D., and Ba, J. Batchensemble: An alternative approach to efficient ensemble and lifelong learning. In *International Conference on Learning Representations*, 2020.

Williams, C. K. and Rasmussen, C. Gaussian processes for regression. In *Neural Information Processing Systems (NeurIPS)*, 1995.

Yoo, D. and Kweon, I. Learning loss for active learning. *2019 IEEE/CVF Conference on Computer Vision and Pattern Recognition (CVPR)*, pp. 93–102, 2019.

Zagidullin, B., Aldahdooh, J., Zheng, S., Wang, W., Wang, Y., Saad, J., Malyutina, A., Jafari, M., Tanoli, Z., Pessia, A., et al. Drugcomb: an integrative cancer drug combination data portal. *Nucleic acids research*, 47(W1):W43–W51, 2019.

Zhang, S., Golbraikh, A., Oloff, S., Kohn, H., and Tropsha, A. A novel automated lazy learning qsar (all-qsar) approach: method development, applications, and virtual screening of chemical databases using validated all-qsar models. *Journal of chemical information and modeling*, 46(5):1984–1995, 2006.

Appendices

A. Related Work

Recently, several novel deep learning-based techniques to estimate uncertainty with a single model have been proposed. For example, Deep Evidential Regression (Amini et al., 2020) is a method for estimating epistemic uncertainty that is based on a parametric estimate of model variance. Orthonormal Certificates, a set of learned features with a suitable loss function, are used in (Tagasovska & Lopez-Paz, 2019). These certificates capture the distance to the training set to learn an estimate of the epistemic uncertainty. This is further studied in Liu et al. (2020) who formalize *distance awareness*, which captures the model’s ability to quantify the distance of a test sample from the training data manifold, as a necessary condition for uncertainty estimation. This distance awareness can be capture with a weight normalization step in training, in addition to using a GP as the output layer. DUN (Antoran et al., 2020) uses the disagreement between the outputs from intermediate layers as a measure of uncertainty. DUQ (van Amersfoort et al., 2020) on the other hand uses two-sided Jacobian regularization on RBF networks (LeCun et al., 1998) for reliable uncertainty estimates.

Wen et al. (2020) present an efficient way of implementing ensembles of neural networks, by using one shared matrix and a rank-1 matrix per member. The weights for each member are then computed as the Hadamard product of the shared matrix and the rank-1 matrix of the member. There has also been extensive work in scaling up Bayesian Neural Networks for high-dimensional data to capture epistemic uncertainty. SWAG (Maddox et al., 2019) fits a Gaussian distribution capturing the SWA (Izmailov et al., 2018) mean and a covariance matrix representing the first two moments of SGD iterated. This distribution is then used as a posterior over the neural network weights. (Dusenberry et al., 2020) parametrize the BNN with a distribution on a rank-1 subspace for each weight matrix, inspired by BatchEnsembles (Wen et al., 2020).

There are also interesting connections between the problem of out-of-distribution generalization arising in sequential model optimization and Bayesian optimization, discussed here, and the possibility of reweighing examples, see Farquhar et al. (2021).

B. Proofs

B.1. Proposition 1

Using equations 4 and 1, along with equations 9 and 7 yield

$$\begin{aligned}
 B(\mathcal{L}, \mathcal{D}_n, x) &= E_f[\mathcal{E}(f, x)] - V(\mathcal{L}, \mathcal{D}_n, x) \\
 &= E_f \left[\int (f(x) - y)^2 dP(y|x) \right] - \mathcal{A}(x) - V(\mathcal{L}, \mathcal{D}_n, x) \\
 &= \int \int (f(x) - y)^2 dP(y|x) dP_{\mathcal{L}}(f(x)|\mathcal{D}_n) - \int (f(x) - \bar{f}(x))^2 dP_{\mathcal{L}}(f(x)|\mathcal{D}_n) - \mathcal{A}(x) \\
 &= \int \left(\int (f(x) - y)^2 dP(y|x) - \int (f(x) - \bar{f}(x))^2 dP(y|x) \right) dP_{\mathcal{L}}(f(x)|\mathcal{D}_n) - \mathcal{A}(x) \\
 &= \int \int (f(x)^2 + y^2 - 2yf(x) - f(x)^2 - \bar{f}(x)^2 + 2f(x)\bar{f}(x)) dP(y|x) dP_{\mathcal{L}}(f(x)|\mathcal{D}_n) - \mathcal{A}(x) \\
 &= \int \int (y^2 - 2yf(x) - \bar{f}(x)^2 + 2f(x)\bar{f}(x)) dP(y|x) dP_{\mathcal{L}}(f(x)|\mathcal{D}_n) - \mathcal{A}(x) \\
 &= \int \left(y^2 - \bar{f}(x)^2 + \int (-2yf(x) + 2f(x)\bar{f}(x)) dP_{\mathcal{L}}(f(x)|\mathcal{D}_n) \right) dP(y|x) - \mathcal{A}(x) \\
 &= \int (y^2 - \bar{f}(x)^2 - 2y\bar{f}(x) + 2\bar{f}(x)^2) dP(y|x) - \mathcal{A}(x) \\
 &= \int (y^2 + \bar{f}(x)^2 - 2y\bar{f}(x)) dP(y|x) - \mathcal{A}(x) \\
 &= \int (y - \bar{f}(x))^2 dP(y|x) - \mathcal{A}(x) = \mathcal{E}(\bar{f}, x)
 \end{aligned}$$

Which concludes the proof.

B.2. Proposition 5

From Equation 15, we get:

$$\begin{aligned}
 \mathcal{E}(Q(Y|x), x) &= KL(P(Y|x)||Q(Y|x)) \\
 &= \log \frac{\sigma_Q(x)}{\sigma_P(x)} + \frac{\sigma_P^2(x) + (f(x) - f^*(x))^2}{2\sigma_Q^2(x)} - \frac{1}{2} \\
 &= \frac{1}{2\sigma_Q^2(x)} l_{MSE}(f(x), f^*(x)) + \log \frac{\sigma_Q(x)}{\sigma_P(x)} + \frac{\sigma_P^2(x) + (f^*(x) - f^*(x))^2}{2\sigma_Q^2(x)} - \frac{1}{2} \\
 &= \frac{1}{2\sigma_Q^2(x)} l_{MSE}(f(x), f^*(x)) + KL(P(Y|x)|\tilde{Q}(Y|x))
 \end{aligned}$$

Which concludes the proof

B.3. Proposition 6

By definition of the total uncertainty:

$$\mathcal{U}(f, x) = \int (f(x) - y)^2 dP(y|x) = E[l_{MSE}(f(x), Y)].$$

Hence, by definition of aleatoric uncertainty:

$$\mathcal{A}(x) = \mathcal{U}(f^*, x) = E[l_{MSE}(f^*(x), Y)].$$

and by definition of epistemic uncertainty

$$\begin{aligned}
 \mathcal{E}(f, x) &= E[(f(x) - y)^2 - (f^*(x) - y)^2] \\
 &= f(x)^2 - f^*(x)^2 - 2(f(x) - f^*(x))E[y] \\
 &= f(x)^2 - f^*(x)^2 - 2(f(x) - f^*(x))f^*(x) \\
 &= l_{MSE}(f(x), f^*(x)).
 \end{aligned}$$

Which concludes the proof.

B.4. Proposition 7

Combining the definition of asymptotic optimality (Equation 6) and Proposition 6, it follows that as the amount of validation data grows to infinity, we have $(e(x) - e^*(x))^2 \rightarrow 0$, where $e^*(x)$ is the Bayes-optimal predictor for the input-target pairs $(x, z = l(f(x), y))$.

By Definition of what is a Bayes Optimal predictor, we have:

$$\begin{aligned}
 e^*(x) &= \arg \min_{\tilde{z}} \int l(\tilde{z}, z) dP(z|x) \\
 &= \arg \min_{\tilde{z}} \int (\tilde{z} - l(f(x), y))^2 dP(y|x).
 \end{aligned}$$

By observing that

$$\frac{\partial \int (\tilde{z} - l(f(x), y))^2 dP(y|x)}{\partial \tilde{z}} = 2 \int (\tilde{z} - l(f(x), y)) dP(y|x)$$

is equal to zero when $\tilde{z} = \int l(f(x), y) dP(y|x)$, and given Proposition 6, we obtain that:

$$e^*(x) = \mathcal{U}(f, x).$$

Meaning that, as the amount of validation data grows to infinity, we get that $e(x) \rightarrow \mathcal{U}(f, x)$; which concludes the proof.

B.5. Proposition 8

We use similar elements of the proof of Proposition 7.

The Bayes-optimal predictor g^* for the input-target pairs $(x, z = \frac{1}{2}(y_1 - y_2)^2)$, is obtained by setting the derivative of $\int(\tilde{z} - \frac{1}{2}(y_1 - y_2)^2)^2 dP(y_1|x) dP(y_2|x)$, with respect to \tilde{z} to zero:

$$\begin{aligned} g^*(x) &= \frac{1}{2} E_{P(y_1|x), P(y_2|x)}[(y_1 - y_2)^2] \\ &= E_{P(y_1|x)}[y_1^2] - E_{P(y_1|x)}[y_1]^2 \quad (\text{i.i.d. assumption}) \\ &= E_{P(y|x)}[(y - E[y|x])^2] \end{aligned}$$

Note that $E_{P(y|x)}[y|x]$, in the case of mean squared error, coincides with $f^*(x)$ (e.g. by using evaluating the derivative again to obtain the minimum). Which means, according to Proposition 7, that $g^*(x) = \mathcal{A}(x)$.

This suffices to show that $a(x)$ is an estimator of $\mathcal{A}(x)$, that converges to $\mathcal{A}(x)$ if the learning algorithm for a is asymptotically optimal, for the same reasons mentioned in the proof of Proposition 7.

C. Pseudo Codes

In this section, we present the pseudo-code of DEUP in two settings: Algorithm 1 illustrates the training procedure when a held-out validation set is available, and Algorithm 2 illustrates how DEUP is used for Active Learning.

Algorithm 1 DEUP with a fixed training set: Training procedure to obtain estimates of epistemic uncertainty

Data: \mathcal{D} training dataset with pairs (x, y) , \mathcal{D}_{out} out-of-sample dataset with pairs (x, y) , to train the uncertainty estimator

a : trained estimator of aleatoric uncertainty (e.g. using Proposition 8, or a constant)

f : predictor trained on \mathcal{D}

e : total uncertainty estimator

Training:

Initialize empty dataset of errors \mathcal{D}_e

for every pair (x, y) in $\mathcal{D} \cup \mathcal{D}_{out}$ **do**

$\mathcal{D}_e \leftarrow \mathcal{D}_e \cup \{(x, (y - f(x))^2)\}$

end

Fit e on \mathcal{D}_e

Evaluation: For every input x , return $e(x) - a(x)$ as an estimator of epistemic uncertainty at x

D. Rejecting Difficult Examples

We adapt the standard OOD rejection task (van Amersfoort et al., 2020; Liu et al., 2020) to measure the Spearman Rank Correlation of the predicted uncertainty with the true generalization error, instead of the OOD Detection AUC. We use MC-Dropout (Gal & Ghahramani, 2016), Deep Ensemble (Lakshminarayanan et al., 2017) and DUQ (van Amersfoort et al., 2020) as the baselines¹. For all the methods, including DEUP we consider two architectures for the main predictor, ResNet-18 and ResNet-50 (He et al., 2016) to study the effect of model capacity.

Training The baselines were trained with the CIFAR-10 training set with 10% set aside as a validation set for hyperparameter tuning. The hyperparameters are presented in Table 3 and Table 4. The hyperparameters not specified are set to the default values. For DEUP, we consider the log-density, model-variance estimate and the seen-unseen bit as the features for the error predictor. The density estimator we use is Masked-Autoregressive Flows (Papamakarios et al., 2017) and the variance estimator used is DUQ (van Amersfoort et al., 2020). Note that x , the input image, is not used as a feature for the error predictor. For training DEUP, the CIFAR-10 training set is divided into 5 folds, with each fold containing 8 unique classes. For each fold, we train an instance of the main predictor, density estimator and model variance estimator on only the corresponding 8 classes. The remaining 2 classes act as the out-of-distribution examples for training the error predictor.

¹MC-Dropout and Deep Ensemble baselines are based on <https://github.com/google/uncertainty-baselines> and DUQ based on <https://github.com/y0ast/deterministic-uncertainty-quantification>

Algorithm 2 DEUP in an active learning setting: Training procedure to acquire more points

Data: \mathcal{D}_{init} initial training dataset with pairs (x, y)
 \mathcal{X} input/search space

 a : estimator of aleatoric uncertainty (e.g. using Proposition 8, or a constant)

 f : main predictor

 e : total uncertainty estimator

 ϕ : extra-feature generator (e.g. with density estimation, variance estimation using a GP or Ensembles, binary feature s - Section 3.3.3)

 acq : acquisition function that proposes new input points x (e.g. Expected Improvement)

Training:

 Initialize empty dataset to train the uncertainty estimator, \mathcal{D}_e

 Initialize $\mathcal{D} = \mathcal{D}_{init}$, the dataset of training points seen so far

Optional: Pre-fill \mathcal{D}_e using initial training data \mathcal{D}_{init}
while stopping criterion not reached **do**
Optional (or every few iterations only): Fit a on \mathcal{D}

 Fit f on \mathcal{D}

 Fit ϕ on \mathcal{D}
 $\mathcal{D}_e \leftarrow \mathcal{D}_e \cup \bigcup_{(x,y) \in \mathcal{D}} \{((x, \phi(x)), (y - f(x))^2)\}$

 Fit e on \mathcal{D}_e
 $x_{acq} \leftarrow acq(\mathcal{X}, f, e - a)$ (can be either a single point, or a batch of points)

 Sample from the ground truth distribution: $y_{acq} \sim P(\cdot | x_{acq})$
 $\mathcal{D}_e \leftarrow \mathcal{D}_e \cup \{((x_{acq}, \phi(x_{acq}), (y_{acq} - f(x_{acq}))^2)\}$
 $\mathcal{D} \leftarrow \mathcal{D} \cup \{(x_{acq}, y_{acq})\}$
end

Using these folds we construct a dataset for training the error predictor, a simple feed forward network. The error predictor is trained with the log targets (i.e. log MSE between predicted and observed error). This helps since the scale of the errors varies over multiple orders of magnitude. We then train the main predictor, density estimator and the variance estimator on the entire CIFAR-10 dataset, for evaluation. The hyperparameters are presented in Table 4. For all models, we train the main predictor for 75 and 125 epochs for ResNet-18 and ResNet-50 respectively. We use SGD with Momentum (set to 0.9), with a multi-step learning schedule with a decay of 0.2 at epochs [25, 50] and [45, 90] for ResNet-18 and ResNet-50 respectively. For all the models we evaluate the Spearman Rank Correlation Coefficient on the SVHN test set.

Table 3. Left: Hyperparameters for training Deep Ensemble (Lakshminarayanan et al., 2017). *Right:* Hyperparameters for training MC-Dropout (Gal & Ghahramani, 2016).

Parameters	Model	
	ResNet-18	ResNet-50
Number of members	5	5
Learning Rate	0.05	0.01

Parameters	Model	
	ResNet-18	ResNet-50
Number of samples	50	50
Dropout Rate	0.15	0.1
L2 Regularization Coefficient	6e-5	8e-4
Learning Rate	0.05	0.01

Ablations We also perform some ablation experiments to study the effect of each feature for the error predictor. The Spearman rank correlation coefficient between the generalization error and the variance feature, V , from DUQ (van Amersfoort et al., 2020) alone is 37.56 ± 0.03 , and the log-density, D , from MAF (Papamakarios et al., 2017) alone is 30.52 ± 0.03 .

Table 5 presents the results for these experiments. We observe that combining all the features performs the best. Also note that using the log-density and variance as features to the error predictor we observe better performance than using them directly, indicating that the error predictor perhaps captures a better target for the epistemic uncertainty. The boolean feature (B) indicating seen examples, discussed in Section 3.3.4, also leads to noticeable improvements.

Table 4. **Left:** Hyperparameters for training DUQ (van Amersfoort et al., 2020). **Right:** Hyperparameters for training DEUP.

Parameters	Model		Parameters	Model	
	ResNet-18	ResNet-50		ResNet-18	ResNet-50
Gradient Penalty	0.5	0.65	Uncertainty Predictor Architecture	[1024] x 5	[1024] x 5
Centroid Size	512	0.1512	Uncertainty Predictor Epochs	100	100
Length scale	0.1	0.2	Uncertainty Predictor LR	0.01	0.01
Learning Rate	0.05	0.025	Main Predictor Learning Rate	0.05	0.01

 Table 5. Spearman Rank Correlation between predicted uncertainty and the true generalization error on OOD data (SVHN) with variants of DEUP with different features as input for the uncertainty predictor. D indicates the log-density from MAF (Papamakarios et al., 2017), V indicates variance from DUQ (van Amersfoort et al., 2020) and B indicates a bit indicating if the data is seen.

Features	Model	
	ResNet-18	ResNet-50
$D+V+B$	42.45 ± 0.04	45.71 ± 0.02
$D+V$	41.72 ± 0.02	44.39 ± 0.03
$V+B$	39.87 ± 0.01	41.65 ± 0.03
$D+B$	40.32 ± 0.03	42.11 ± 0.02

E. DEUP in the presence of aleatoric uncertainty

In the presence of aleatoric uncertainty, we have seen that DEUP’s error predictor e is an estimate of the total uncertainty, rather than the epistemic uncertainty. However, if we have access to an estimator of aleatoric uncertainty a , then $e - a$ becomes an estimator of epistemic uncertainty. To show the difference in behavior of DEUP when there is aleatoric uncertainty, we consider, a modified version of the experiment in Section 5.1.1, with a non-deterministic oracle (ground truth function). Because of the noisy training dataset, GP conflates epistemic and aleatoric uncertainty, which makes the gap between the predicted epistemic uncertainty (as measured by the GP variance) and the true epistemic uncertainty (as measured by the MSE between the GP mean and the noiseless ground truth function) higher than in the deterministic setting of Section 5.1.1.

Similarly, in order to train DEUP’s uncertainty estimator, more out-of-sample data is needed compared to the noiseless setting. If figure 5, we consider the setting described in Section 3.2.2, and train a separate predictor on the targets mentioned in Proposition 8 to estimate the aleatoric uncertainty (which boils down to the variance of the ground-truth function). Because these targets are themselves noisy, we chose a simple linear regressor as the estimator of aleatoric uncertainty, to avoid overfitting to the noise.

A key distinction of this setting, is that DEUP’s training data are themselves noisy, which makes it important to use more out-of-sample data to obtain reasonable total uncertainty estimates (from which we subtract the estimates of the aleatoric uncertainty).

F. Sequential Model Optimization Experiments

We use BoTorch² (Balandat et al., 2020) as the base framework for our experiments.

F.1. Additional details for the one-dimension function

In Figure 6, we show the results of DEUP-EI, compared to GP-EI, MCDropout-EI and Ensembles-EI. Because MCDropout and Ensembles are trained on in-sample data only, they are unable to generalize their uncertainty estimates, which makes them bad candidates for Sequential Model Optimization, because they are easily stuck in local minima, and require many iterations before the acquisition function gives more weight to the predicted uncertainties than the current maximum.

For Random acquisition, we sampled for different seeds 56 points, and used the (average across the seeds of the) maximum

²<https://botorch.org/>

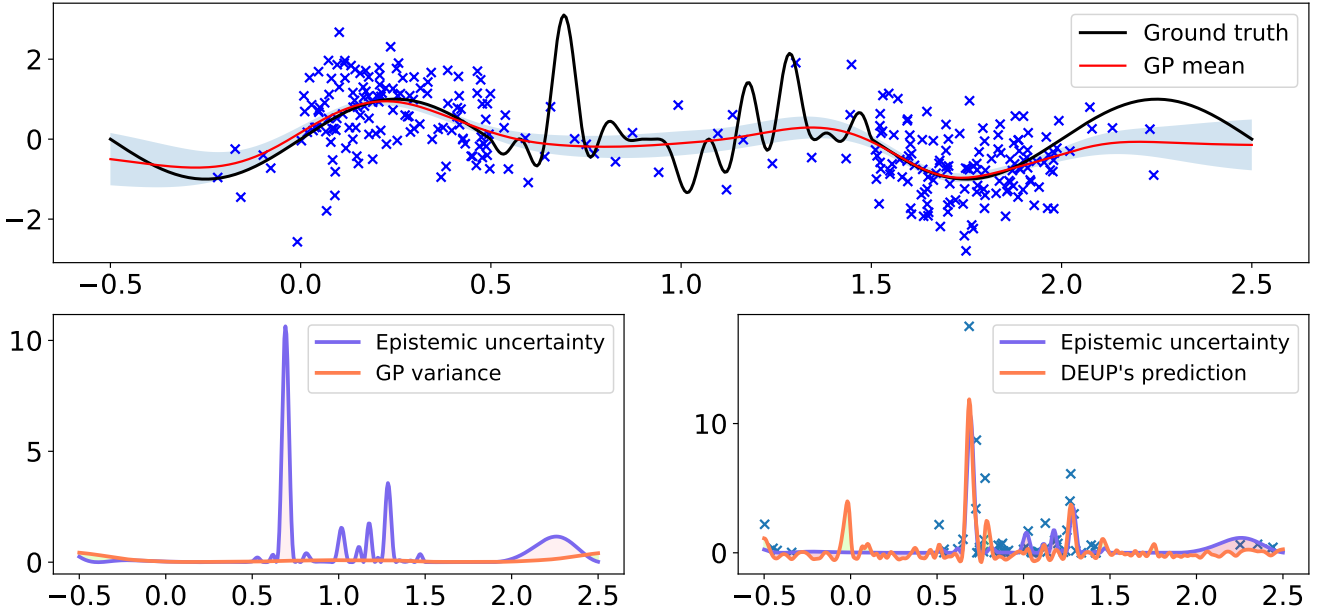


Figure 5. Top. A GP is trained to regress a function using noisy samples. GP uncertainty (model standard deviation) is shaded in blue. Bottom left. Using GP variance as a proxy for epistemic uncertainty misses out on more regions of the input space, when compared to Figure 1. Bottom right. Using additional out-of-sample data in low density regions, a second GP is trained to predict the generalization error of the first GP (total uncertainty). Using second samples from the oracle for each of the training points, a linear regressor fits the training pairs $(x, \frac{1}{2}(y_1 - y_2)^2)$ to estimate the pointwise aleatoric uncertainty (constant in this case). The aleatoric uncertainty is subtracted from DEUP's (second GP) predictions to obtain more accurate epistemic uncertainty. Note that no constraint is imposed on DEUP's outputs, which explains the predicted negative values for uncertainties. In practice, if these predicted uncertainties were to be used, (soft) clipping should be used.

of the first 6 values as the first value in the plots (Figures 3 and 6). Note that because the function is specifically designed to have multiple local maxima, GP-EI also required more optimization steps, and actually performed worse than random acquistion

Note that DEUP uncertainty estimator was trained using Algorithm 2. We found that the optional step of pre-filling the uncertainty estimator dataset \mathcal{D}_e was important given the low number of available training points. We used half the initial training set (randomly chosen) as in-sample examples to train a main predictor and an extra-feature generator, and the other half as out-of-sample examples to provide instances of high epistemic uncertainty to train an uncertainty predictor; we repeated the procedure by alternating the roles of the two halves of the dataset. We repeated the whole procedure twice using a new random split of the dataset, thus ending up with 4 training points in \mathcal{D}_e for every initial training point in \mathcal{D}_{init} .

The error predictor is trained with the log targets (i.e. log MSE between predicted and observed error). This helps since the scale of the errors varies over multiple orders of magnitude.

As a stationarizing feature, we used the variance of a GP fit on the available data at every step. We found that the binary feature and density estimates were redundant with this feature and didn't improve the performance as captured by the number of additional function calls. We used a GP for DEUP uncertainty estimator. Using a neural net provided similar results, but was computationally more expensive. We used a 3-hidden layer neural network, with 128 neurons per layer and ReLU activation function, and Adam (Kingma & Ba, 2015) with a learning rate of 10^{-3} (and default values for the other hyperparameters) to train the main predictor for DEUP-EI (in order to fit the available data). The same network architecture and learning rate were used for the Dropout and Ensemble baselines. We used 3 networks for the Ensemble baseline, and a dropout probability of 0.3 for the Dropout baseline, with 100 test-time forward passes to compute uncertainty estimates.

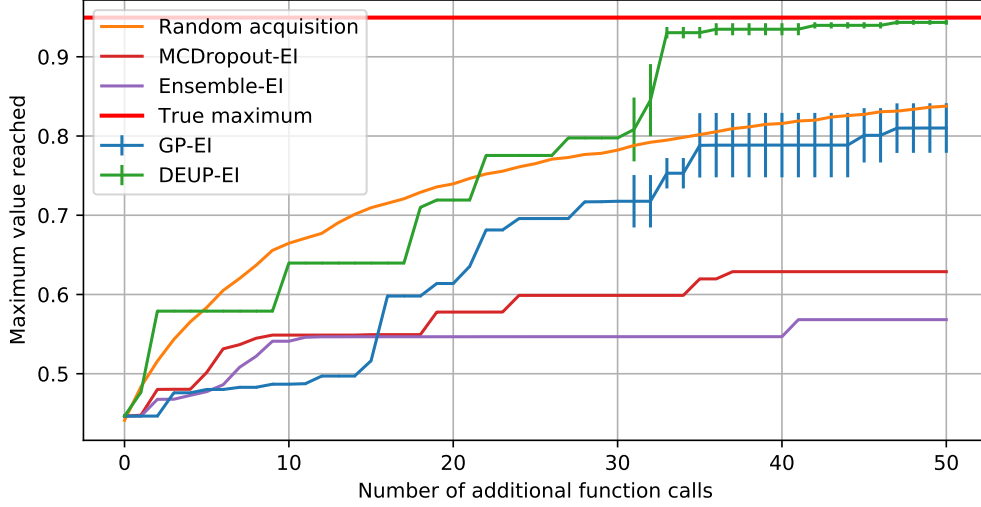


Figure 6. Maximum value reached by the different optimization methods, for the same function as in Figure 3. In each run, all the methods start with the same initial of 6 points. Error bars are omitted for MCDropout, Ensemble, and Random acquisition for clarity.

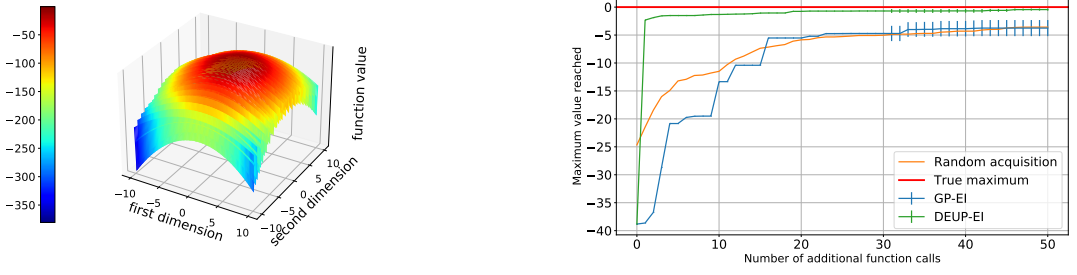
F.2. Two-dimensional function

To showcase DEUP’s usefulness for Sequential Model Optimization in higher dimension, we consider the optimization of the Levi N.13 function, a known benchmark for optimization. The function f takes a point (x, y) in 2D space and returns:

$$f(x, y) = -(\sin^2(3\pi x) + (x - 1)^2(1 + \sin^2(3\pi y)) + (y - 1)^2(1 + \sin^2(2\pi y)))$$

We use the box $[-10, 10]^2$ as the optimization domain. In this domain, the maximum of the function is 0, and it is reached at $(1, 1)$. The function has multiple local maxima, as shown in Figure 7(a).

Similar to the previous one-dimensional function, MCDropout and Ensemble provided bad performances and are omitted from the plot in 7(b). We used the same setting and hyperparameters for DEUP as for the previous function. DEUP-EI is again the only method that reaches the global maximum consistently in under 56 function evaluations.



(a) Visualization of the function

(b) Comparisons with GP-EI and Random acquisition

Figure 7. Sequential Model Optimization on the Levi N.13 function

G. Reinforcement Learning Experiments

For RL experiments, we used *bsuite* (Osband et al., 2020) that is a collection of carefully designed RL environments. *bsuite* also comes with a list of metrics which aim to evaluate RL agents from different aspects. We compare the agents based on the *basic* metric and average regret as they capture both sample complexity and final performance. The default DQN

agent is used as the base of our experiments with a 3 layer fully-connected (FC) neural network as its Q-network. For the Bootstrapped DQN baseline, we used the default implementation provided by *bsuite*. To implement DQN + MC-Dropout, following the implementation from [Gal & Ghahramani \(2016\)](#), two dropout layers with dropout probability of 0.1 are used before the second and the third FC layers. In order take an action, the agent performs a single stochastic forward pass through the Q-network, which is equivalent to taking a sample from the posterior over the Q-values, as done in Thompson sampling, an alternative to ϵ -greedy exploration.

As a density estimator, we used a Kernel Density Estimator (KDE) with a Gaussian kernel and bandwidth of 1 to map states to densities. This KDE is fit after each 10000 steps (actions) with a batch of samples from the replay buffer (which is of size 10000). The uncertainty estimator network (E-network) has the same number of layers as the Q-network, with an additional Softplus layer at the end. All other hyperparameters are the same as the default implementation by [Osband et al. \(2020\)](#).

Algorithm 3 DEUP-DQN

Initialize replay buffer \mathcal{D} with capacity \mathcal{N}
 $Q_\theta(s, a)$: state-action value predictor
 $E_\phi(\log d)$: uncertainty estimator network, which takes the log-density of the states as the input
 $d(s)$: Kernel density estimator (KDE)
K: KDE fitting frequency
W: Number of warm-up episodes
for $episode=1$ to M **do**
 set s_0 as the initial state
 for $t=1$ to $max\text{-}steps\text{-}per\text{-}episode$ **do**
 with probability ϵ : take a random action, **otherwise**:
 if $episode \leq W$: $a = max_a Q_\theta(s_t, a)$, **else**: $a = max_a [Q_\theta(s_t, a) + \kappa \times E_\phi(\log d(s_t))(a)]$
 store (s_t, a_t, r_t, s_{t+1}) in \mathcal{D}
 Sample random minibatch B of transitions (s_j, a_j, r_j, s_{j+1}) from \mathcal{D}
 if s_j is a final state: $y_j = r_j$, **else**: $y_j = r_j + \gamma max_a Q(s_{j+1}, a)$
 Update Q-network:
 $\theta \leftarrow \theta + \alpha_Q \cdot \nabla_\theta \mathbb{E}_{(s, a) \sim B} [(y_j - Q_\theta(s, a))^2]$
 Update E-network:
 $\phi \leftarrow \phi + \alpha_E \cdot \nabla_\phi \mathbb{E}_{(s, a) \sim B} \left[\left[(y_j - Q_\theta(s, a))^2 - E_\phi(\log d(s_t))(a) \right]^2 \right]$
 if $mod(total\text{-}steps, K) = 0$: fit the KDE d on the states of \mathcal{D}
 end
end

H. Drug Combination Experiments

To validate DEUP’s uncertainty estimates in a real-world setting, we measured its performance on a regression task predicting the synergy of drug combinations. While much effort in drug discovery is spent on finding novel small molecules, a potentially cheaper method is identifying combinations of pre-existing drugs which are synergistic (i.e., work well together). Indeed, drug combinations are the current standard-of-care for a number of diseases including HIV, tuberculosis, and some cancers ([Cihlar & Fordyce, 2016](#); [Organization & Initiative, 2010](#); [Mokhtari et al., 2017](#)).

However, due to the combinatorial nature of drug combinations, identifying pairs exhibiting synergism is challenging. Compounding this problem is the high monetary cost of running experiments on promising drug combinations, as well as the length of time the experiments take to complete. Uncertainty models could be used by practitioners downstream to help accelerate drug combination treatment discoveries and reduce involved development costs.

To test DEUP’s performance on this task we used the DrugComb and LINCS L1000 datasets ([Zagidullin et al., 2019](#); [Subramanian et al., 2017](#)). DrugComb is a dataset consisting of pairwise combinations of anti-cancer compounds tested on various cancer cell lines. For each combination, the dataset provides access to several synergy scores, each indicating whether the two drugs have a synergistic or antagonistic effect on cancerous cell death. LINCS L1000 contains differential gene expression profiles for various cell lines and drugs. Differential gene expressions measure the difference in the amount

of mRNA related to a set of influential genes before and after the application of a drug. Because of this, gene expressions are a powerful indicator of the effect of a single drug at the cellular level.

In our experiments, each drug is represented by its Morgan fingerprint (Morgan, 1965)³ (with 1,024 bits and a radius of 3) as well as two differential gene expression profiles (each of dimension 978) from two cell lines (PC-3 and MCF-7). In order to use gene expression features for every drug, we only used drug pairs in DrugComb where both drugs had differential gene expression data for cell lines PC-3 and MCF-7.

We first compared the quality of DEUP’s uncertainty estimations to other uncertainty estimation methods on the task of predicting the combination sensitivity score (Malyutina et al., 2019) for drug pairs tested on the cell line PC-3 (1,385 examples). We evaluated the uncertainty methods using a train, validation, test split of 40%, 30%, and 30%, respectively. The underlying model used by each uncertainty estimation method consisted of a *single drug* fully connected neural network (2 layers with 2048 hidden units and output of dimension 1024) and a *combined drug* fully connected neural network (2 layers, with 128 hidden units). The embeddings of an input drug pair’s drugs produced by the *single drug* network are summed and passed to the *combined drug* network, which then predicts final synergy. By summing the embeddings produced by the *single drug* network, we ensure that the model is invariant to permutations in order of the two drugs in the pair. The models were trained with Adam (Kingma & Ba, 2015), using a learning rate of 1e-4 and weight decay of 1e-5. For MC-Dropout we used a dropout probability of 0.1 on the two layers of the *combined drug* network and 3 test-time forward passes to compute uncertainty estimates. The ensemble used 3 constituent models for its uncertainty estimates. Both Ensemble and MC-Dropout models were trained with the *MSE* loss.

Algorithm 4 DEUP for Drug Combinations

Data: \mathcal{D} dataset of pairwise drug combinations, along with synergy scores $((d_1, d_2), y)$

Initialization:

Split training set into two halves, *in-sample* \mathcal{D}_{in} and *out-of-sample* \mathcal{D}_{out}

$f_\mu(d_1, d_2)$: $\hat{\mu}$ predictor which takes a pair of drugs as input

$f_\sigma^{in}(d_1, d_2)$: In-sample $\hat{\sigma}_{in}$ error predictor

$f_\sigma^{out}(d_1, d_2)$: Out-of-sample $\hat{\sigma}_{out}$ error predictor

Training:

while training not finished **do**

In-sample update

 Get an *in-sample* batch $(d_{1,in}, d_{2,in}, y_{in}) \sim \mathcal{D}_{in}$

 Predict $\hat{\mu} = f_\mu(d_{1,in}, d_{2,in})$ and *in-sample* error $\hat{\sigma}_{in} = f_\sigma^{in}(d_{1,in}, d_{2,in})$

 Compute $NLL: \frac{\log(\hat{\sigma}_{in}^2)}{2} + \frac{(\hat{\mu} - y_{in})^2}{2\hat{\sigma}_{in}^2}$

 Backpropagate through f_μ and f_σ^{in} and update.

Out-of-sample update

 Get an *out-of-sample* batch $(d_{1,out}, d_{2,out}, y_{out}) \sim \mathcal{D}_{out}$

 Estimate $\hat{\mu} = f_\mu(d_{1,out}, d_{2,out})$ and *out-of-sample* error $\hat{\sigma}_{out} = f_\sigma^{out}(d_{1,out}, d_{2,out})$

 Compute $NLL: \frac{\log(\hat{\sigma}_{out}^2)}{2} + \frac{(\hat{\mu} - y_{out})^2}{2\hat{\sigma}_{out}^2}$

 Backpropagate through f_σ^{out} and update.

end

The DEUP model we used outputs two heads $[\hat{\mu} \hat{\sigma}]$ and is trained with the $NLL \frac{\log(\hat{\sigma}^2)}{2} + \frac{(\hat{\mu} - y)^2}{2\hat{\sigma}^2}$ in a similar fashion as in (Lakshminarayanan et al., 2017). To obtain a predictor of the out-of-sample error, we altered our optimization procedure so that the μ and σ heads were not backpropagated through at all times. Specifically, we first split the training set into two halves, terming the former the in-sample set \mathcal{D}_{in} and the latter the out-of-sample set \mathcal{D}_{out} . We denote as f_σ^{in} the in-sample error predictor and f_σ^{out} the out-of-sample error predictor. f_σ^{out} is used to estimate total uncertainty. Note that in this setting, f_σ^{out} predicts the square root of the epistemic uncertainty ($\hat{\sigma}_{out}$) rather than the epistemic uncertainty itself ($\hat{\sigma}_{out}^2$).

In our experiments, an extra bit is added as input to the model in order to indicate whether a given batch is from \mathcal{D}_{in} or

³The Morgan fingerprint represents a molecule by associating with it a boolean vector specifying its chemical structure. Morgan fingerprints have been used as a signal of various molecular characteristics to great success (Ballester & Mitchell, 2010; Zhang et al., 2006).

\mathcal{D}_{out} . Through this, the same model is used to estimate f_σ^{in} and f_σ^{out} with the model estimating f_σ^{in} when the bit indicates an example is drawn from \mathcal{D}_{in} and f_σ^{out} otherwise. When the batch is drawn from \mathcal{D}_{in} , both heads are trained using NLL using a single forward pass. However, when the data is drawn from \mathcal{D}_{out} only the $\hat{\sigma}$ head is trained. To do this, we must still predict $\hat{\mu}$ in order to compute the NLL. But the $\hat{\mu}$ predictor f_μ must be agnostic to the difference between \mathcal{D}_{in} and \mathcal{D}_{out} . To solve this, we perform two separate forward passes. The first pass computes $\hat{\mu}$ and sets the indicator bit to 0 so f_μ has no notion of \mathcal{D}_{out} , while the second pass computes $\hat{\sigma}$, setting the bit to 1 to indicate the true source of the batch. Finally, we backpropagate through the $\hat{\sigma}$ head only. The training procedure is described in Algorithm 4

We report several measures for the quality of uncertainty predictions on a separate test set in Table 2. For each model, we computed the correlation between the residuals of the model $|\hat{\mu} - y|$ and the predicted uncertainty $\hat{\sigma}$. We then determined an upper bound for this correlation by computing the correlation between the predicted uncertainties $\hat{\sigma}$ and samples from the corresponding Gaussians $\mathcal{N}(0, \hat{\sigma})$ (5 samples for each example in the test set). We then report the ratio between the correlation $Corr(\text{residual}, \hat{\sigma})$ and the upper bound.

Predicted $\hat{\mu}$ and uncertainty estimates can be visualized in Figure 8 for different models. MC-dropout and Ensemble consistently underestimate uncertainty, while the out-of-sample uncertainties predicted by DEUP are much more consistent with the order of magnitude of the residuals.

Finally, we note that in the context of drug combination experiments, aleatoric uncertainty could be estimated by having access to replicates of a given experiment (c.f. Proposition 8), allowing us to subtract the aleatoric part from the out-of-sample uncertainty, leaving us with the epistemic uncertainty only.

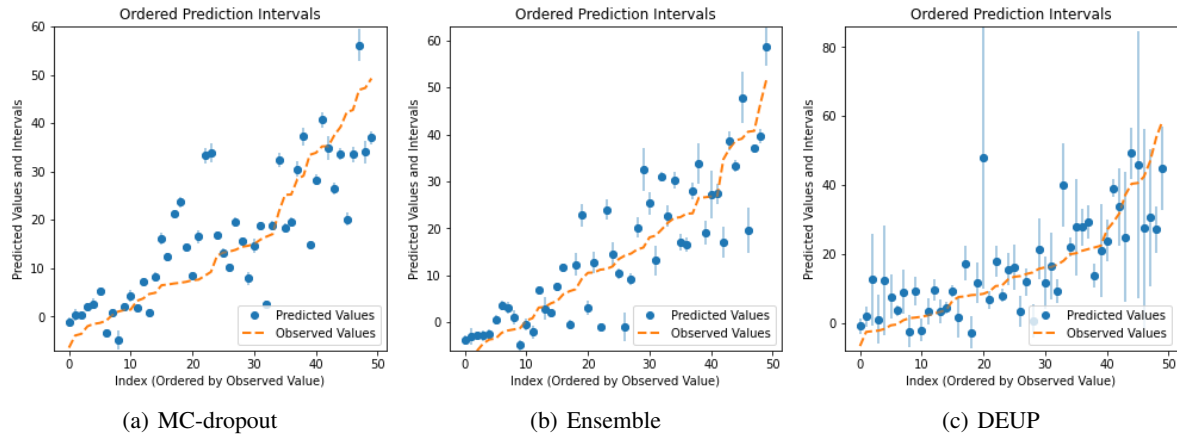


Figure 8. Predicted mean and uncertainty for different models on a separate test set. 50 examples from the test set are ordered by increasing value of true synergy score (orange). Model predictions and uncertainties are visualized in blue. MC-Dropout and Ensemble consistently underestimate the uncertainty while DEUP seems to capture the right order of magnitude.